18. An Eigenstructure Assignment Approach (2)

Jesús M. de la Cruz[1], Pablo Ruipérez[2] and Joaquín Aranda[2]

Abstract. In this chapter the Eigenstructure Assignment Method is applied to the Research Civil Aircraft Model (RCAM) benchmark problem. The design is done by making use of the classical approach which consists of splitting up the controller into two parts, a longitudinal and a lateral controller, and in using the standard inner-outer loop control structure. This method allows us to directly satisfy specifications in terms of transient response and modes decoupling. However, it does not cope directly with system uncertainties. In order to cope with robustness, measurements of multiloop gain and phase margins are used in the choice of a robust eigenstructure. Both channels make use of a constant gain matrix in the inner loop and a scalar gain in the outer loop. In spite of the controller simplicity, good performance and robustness results are obtained, although robustness may be increased by means of gain scheduling with respect to airspeed.

18.1 Introduction

The eigenstructure technique has been widely applied to the design of flight control systems and it is a well-known fact that its use requires an in-depth knowledge of the system to be controlled [11]. Although this method is not intended to deal with robustness, many robustification procedures have been proposed [155]. Here the eigenstructure is chosen so that good multiloop gain and phase stability margins are obtained.

The chapter is organised in the following way. Section 18.2 describes the controller structure used. The controller has been decoupled into the longitudinal and the lateral channels. Both have been designed according to an inner/outer loop control structure. The inner loop controllers are designed following the eigenstructure method. A constant gain matrix is used in both channels. The outer loop only uses a scalar gain that is calculated by means of the root locus method.

[1]Dpt. Informática y Automática. Facultad de Ciencias Físicas. Universidad Complutense. 28040-Madrid. Spain. (Funded by project CICYT TAP94-0832-C02-01).
[2]Dpt. Informática y Automática. Facultad de Ciencias. U.N.E.D. 28040-Madrid. Spain.

Section 18.3 deals with the way the RCAM design criteria are translated into the desired eigenstructure.

Section 18.4 describes the design cycle. The linear model of the plant is analysed and the most appropriate eigenstructure is chosen. Next, the feedback controller is obtained and the performance of the closed-loop system for the linear models is analysed. Multiloop gain and phase margins are used to measure robustness and to guide eigenstructure choice.

In section 18.5 the verification of all the design specifications with the nonlinear system is presented. Simulations for the worst possible combinations of delay, mass and centre of gravity are given.

In section 18.6 the results of the automated evaluation procedure are given.

The theory has been presented in chapter 3. More details, including program code for the design written in Matlab can be found in [52]

18.2 Selection of the controller architecture

We make use of the classical approach consisting of splitting up the controller into two parts: a longitudinal and a lateral controller. Both of them have been designed in two stages: the inner loop and the outer loop. The function of the inner loop is to make the aircraft easy and pleasant to fly, and it is often called a stability augmentation system. The outer loop function is to replace the pilot for certain flight manoeuvres such as maintaining height and speed, turning onto a specified heading, climbing at a specified rate, etc.

Figure 18.1 shows the structure of the longitudinal controller, and figure 18.2 shows the structure of the lateral controller.

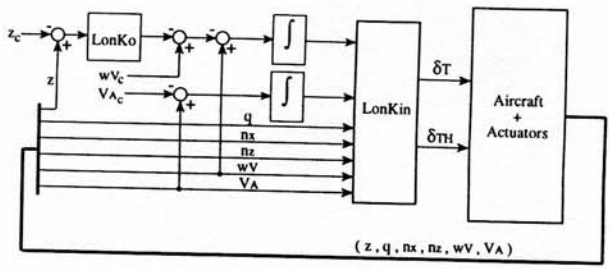

Figure 18.1: Longitudinal controller

18.2.1 Longitudinal controller

The choice of the signals to be used in a design is based on the analysis of the system, the specifications and the design method.

Measurement signals

Table 18.1 shows the measurements as used by the longitudinal controller.

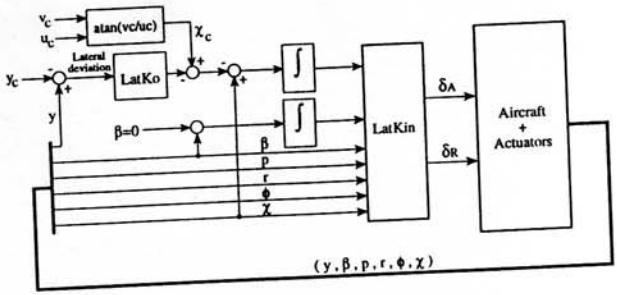

Figure 18.2: Lateral controller

Inner Loop controller	
q	Pitch rate
n_x	Horizontal load factor
n_z	Vertical load factor
w_V	z component of inertial velocity
V_A	Air speed
Outer Loop controller	
z	z position of aircraft CoG

Table 18.1: Longitudinal measurements used

Although in the inner loop only four measurements are needed to assign four eigenvalues, two for the short period and two for the phugoid, we make use of five in order to prevent the slower mode of the actuators (that of the throttle) from becoming unstable, see [52].

Finally, the outer loop provides altitude tracking by adding a feedback of the altitude z.

Actuator signals

These signals are the elevator deflection or tailplane deflection δ_T, and throttle position δ_{TH}.

Reference signals

The selection of signals chosen as references has been guided by the specifications given as design criteria, see §18.3. The selected ones are the reference velocity w_{Vc} and the reference airspeed V_{Ac} for the inner loop, and the reference position z_C for the outer loop.

Controller structure

The inner loop controller has a static gain matrix acting on the five chosen measured signals and on the integral of the errors of the commanded variables w_V and V_A, in the order here specified. The two integrators result in two additional states that must be incorporated into the linear model for the controller design. The outer loop has a proportional action acting on the altitude error. No integral action is needed here to avoid steady state errors related to altitude step commands or disturbances, since the altitude dynamics include a pole at the origin. The output of the outer loop acts as a reference for w_V.

18.2.2 Lateral Controller

The lateral controller has a structure analogous to the longitudinal controller.

Measurement signals

Table 18.2 shows the measurements as used by the lateral controller.

Inner Loop controller	
β	Angle of sideslip
p	Roll rate
r	Yaw rate
ϕ	Roll angle
χ	Inertial track angle
Outer Loop controller	
Δy	Lateral deviation

Table 18.2: Lateral measurements used

Actuator signals

These signals are the aileron deflection δ_A, and rudder deflection δ_R.

Reference signals

Again, the selection of references has been guided by the specifications given as design criteria, see §18.3. Those selected are the lateral deviation for the outer loop, and the inertial track angle χ_C and sideslip angle β_C for the inner loop. χ_C is not given as a reference signal but it is obtained from the reference velocity components u_C and v_C as $\text{atan}(v_C/u_C)$. β_C has a null constant reference value in order to keep β always close to zero.

Controller structure

The inner loop controller has a static gain acting on the five chosen signals measured, and on the integral of the errors of the commanded variables β and

χ, in the order specified here. The introduction of two integrators results in two additional states that must be incorporated into the linear model for the controller design. The outer loop has a proportional action acting on the lateral error. No integral action is required here to avoid steady state errors relating to lateral step commands or disturbances, since the lateral dynamics include a pole at the origin. The output of the outer loop acts as a reference for the inertial track angle.

18.3 Translation of design criteria into method dependent objectives

Out of the five classes of design criteria given in chapter 14, for the RCAM design, the performance criteria are the most significant. These criteria are given in terms of transient response characteristics to command signals and cross coupling constraints. The main characteristic of the eigenstructure assignment method is that it allows the designer to satisfy specifications directly in terms of transient response and mode decoupling. Then, these are the most suitable criteria to be used as a guide in the design phase.

Our design is based mainly on these criteria, but we made use of linear and non-linear closed-loop time responses and robust analysis tools as a guide in the selection of the eigenstructure.

18.3.1 Performance Criteria

The performance criteria can be classified into two groups: longitudinal and lateral. We discuss separately for each group the way in which the specifications have been incorporated into the design.

Longitudinal specifications

There are command response specifications in terms of overshoot, rise time and settling time for three commanded signals: airspeed, flight path angle and altitude. These specifications provide a lower limit for the damping ratio and natural frequency of second order modes and for the time constant of first order modes coupled with the signals.

The flight path angle γ is neither available as an output nor as a reference signal. To cope with this situation we use the relationship $\sin(\gamma) = -w_V/V$, where V is the total inertial velocity. Therefore, for constant inertial velocity the flight path angle may be controlled by means of w_V. This leads us to an interpretation of the specifications in terms of commands in w_{Vc}. We add a vertical velocity error integrator state to get good low-frequency tracking.

We add an outer loop for tracking the reference altitude. A signal proportional to the altitude error is used as a reference signal for w_V. The proportional

gain is calculated using the root locus method in such a way that it fulfils the transient criteria.

The specification of decoupling between airspeed and altitude may be obtained by decreasing cross-coupling between V_A and w_V.

Lateral specifications

There are now two command signal specifications (heading angle and lateral deviation) in terms of transient response characteristics that may be transformed into bounded eigenvalues. The remaining specifications are given in terms of behaviour in case of engine failure and under disturbances.

The heading angle is a lateral motion state but it is neither available as an output nor as a reference. Instead, we make use of the inertial track angle that is an output signal and is related to the heading angle by means of the equation $\chi = \psi + \beta_V$. Although there is no reference signal for χ, such a signal may be obtained from the reference velocity components u_C and v_C by means of equation $\chi_C = \tan^{-1}(v_C/u_C)$. An integrator is introduced to eliminate sideslip errors, where the command signal for β is chosen as 0. Doing so, we cope with the safety criteria of keeping β minimised at all times. An inertial track angle error integrator is also introduced in order to avoid heading angle steady state errors.

The lateral deviation is controlled in the outer loop. A signal proportional to the lateral error is used as a reference signal for the inertial track angle. The proportional gain is calculated using the root locus method in such a way that it fulfils the transient criteria.

The engine failure requirements can not be easily interpreted in terms of eigenvalue and eigenvector specifications and shall not be tested before the phase of analysis of simulation results. However, the requirement of keeping sideslip angle to a minimum in case of engine failure can be translated into a specification of decoupling between the eigenvalues related with the roll motion and those related with the lateral velocity.

18.3.2 Robustness criteria

The eigenstructure method is not a robust control method and, although many different algorithms have been proposed to enhance the robustness, no method will be used here. However, we make use of the stability margins given in chapter 3 to measure the robustness of the feedback system. For a chosen eigenstructure the stability margins are measured and the eigenstructure changed to get better stability margins. After a few steps a suitable eigenstructure is selected.

18.3.3 Other criteria

The ride quality criteria, safety criteria and control activity criteria can not be incorporated in an *ad hoc* manner into the eigenstructure method. As done

with robustness, they will be analysed in the course of the analysis of results phase and physical relations between their behaviour and the eigenstructure achieved will be established in order to cope with them. In the selection of the eigenvalues we should have in mind to assign the mode values close to the open-loop aircraft modes to minimise the control activity.

18.4 Design cycle and controller derivation

The design cycle is summarised in the following scheme

1. Analysis of the linear and non-linear model of the plant.
2. Selection of the eigenstructure and gain calculation.
3. Analysis of the open and closed-loop system (linear and non linear model).
4. Robustification procedure (iterate).
5. Iterate 1 - 4.

As we have seen in the previous section, among all the design criteria only those of the performance criteria related to the transient response of the system can be interpreted almost directly in terms of eigenstructure. The rest of them must be analysed after an eigenstructure has been chosen and the controller found. From this analysis another eigenstructure will be chosen and so on. That has been the most consuming time task. A robustification procedure or any other form of "optimal" solution may help to break the iterative procedure.

We will now explain the method we have used to select an eigenstructure.

- We analysed the design criteria and the coupling of the modes of the plant with the states, the inputs and the outputs. This analysis was used as a guide in choosing the outputs for feedback and the eigenstructure. After selecting the outputs to be used for feedback the integrators were added to the loop.

- We chose a set of eigenvalues that fulfilled the transient response limits in accordance with the requirements and were close to the natural aircraft modes. After that, their associated eigenvectors were chosen to get the desired decoupling between the modes.

- With the eigenstructure chosen, we computed the feedback gain and analysed:

  - the stability (since one of the non-assigned eigenvalues might become unstable or badly damped) and the stability margins
  - the time response of the system
  - the decoupling of the obtained modes

Now the cycle begins. New outputs and/or eigenstructure must be chosen to improve the results obtained. We have first selected an eigenstructure that provides acceptable design criteria. We have tested different eigenvalues with fixed eigenvectors. Once the eigenvalues that give better stability margins have been chosen, the eigenvectors have been changed to try to improve robustness and, when necessary, decoupling. After a few steps we convinced ourselves that the chosen eigenvectors could not be improved.

18.4.1 Longitudinal controller

Longitudinal model

The non-linear model is used to generate linear models for control law design and to generate non-linear time histories for evaluating control designs. Once a trim condition is established for the non-linear aircraft model within the simulation environment, a linear model is generated to capture the perturbational dynamics around the equilibrium point. The model has been linearised around the following operating condition: $V = 80$ m/s, $h = 1000$ m, $mass = 120000$ kg, $cgx = 0.23$ and $cgz = 0.1$. The aerodynamic model is augmented with first order actuator models. Two integrated error states are added to the linearised model, one for w_V and another for V_A. The number of outputs is now increased by two and the eigenvalues for the modes of the integrators may be specified. The maximum allowed transport time delay of 0.10 s is added to the model with a first order Padé approximation.

Inner loop controller design

As mentioned in chapter 3 we can specify as many closed-loop eigenvalues as outputs for feedback used. Therefore, only four measurements are needed to specify the phugoid and short period modes. However, we used five measurements so that the slower mode of the actuators (that of the throttle) is specified, in order to avoid it becoming unstable.

Mode	Phugoid	Short Period	Throttle	$\int w_V$	$\int V_A$
Eigenvalues	-0.4376 $\pm 0.0624i$	-0.9059 $\pm 0.4388i$	-0.5	-2.0000	-1.9000
q	x x	1 x	x	x	x
θ	x 1	x x	x	x	x
u_B	1 x	0 0	x	0	x
w_B	0 0	x 1	x	x	0
X_T	x x	x x	x	x	x
X_{TH}	x x	x x	1	x	x
$delay\ \delta_T$	x x	x x	x	x	x
$delay\ \delta_{TH}$	x x	x x	x	x	x
$\int w_V$	0 0	x x	x	1	0
$\int V_A$	x x	0 0	x	0	1

Table 18.3: Desired eigenstructure of the longitudinal closed-loop system

Table 18.3 shows the eigenstructure chosen for the system. The state components are given in the first column, where X_T is the state corresponding to the first order tailplane model and X_{TH} the state corresponding to the first order engine model. The first row shows the desired eigenvalues, and the desired eigenvectors are shown underneath, where the symbol "x" represents the unspecified elements in the eigenvectors. The resulting gain is:

$$LonK_{in} = \begin{bmatrix} 0.4755 & 0.0532 & -0.0838 & -0.0169 & -0.0055 & -0.0033 & -0.0014 \\ 0.0455 & -1.3063 & -0.3047 & -0.0152 & -0.1221 & 0.0004 & -0.0227 \end{bmatrix}$$

Loop stability margins

Figures 18.3 and 18.4 show the singular value plots of the sensitivity function S, the complementary sensitivity function T and the balanced sensitivity function $S+T$ at the actuator inputs and at the sensor outputs. Tables 18.4 and 18.5 show the gain and phase margins obtained from the sensitivity functions.

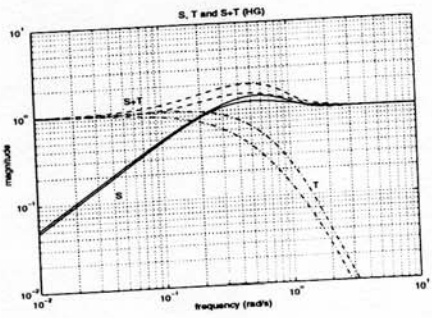

Figure 18.3: Longitudinal inner loop singular values of the input sensitivity functions

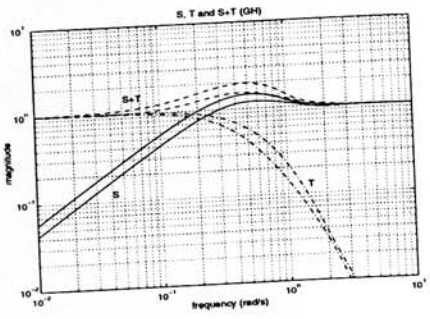

Figure 18.4: Longitudinal inner loop singular values of the output sensitivity functions

Function	$\overline{\sigma}$	ω	$K_m = 1/\overline{\sigma}$	Gain margin (dB)	Phase margin (deg)
S	1.42	0.57	0.70	[-4.6,10.6]	±41.2
T	1.03	0.09	0.98	[-29.7,5.9]	±57.8
$S+T$	1.96	0.48	0.51	[-9.8,9.8]	±54.1

Table 18.4: Longitudinal inner loop stability margins at the inputs

Function	$\overline{\sigma}$	ω	$K_m = 1/\overline{\sigma}$	Gain margin(dB)	Phase margin (deg)
S	1.47	0.54	0.68	[-4.5,10.0]	±39.9
T	1.00	0.02	1.00	[-54.4,6.0]	±59.9
$S+T$	1.96	0.46	0.51	[-9.8,9.8]	±54.1

Table 18.5: Longitudinal inner loop stability margins at the outputs

Good stability margins are obtained, but we must remember that these margins are conservative, and even better stability margins should be expected.

Outer loop controller design

Choosing $LonK_o = 0.1027$, the slower roots are $-0.14 \pm 0.14i$, having a rise time of 11 s, which is less than the specified rise time for an altitude command (15 s), and a settling time of 35.4 s which is well below the required 45 s. The gain margin for the outer loop is 13 dB at $w = 0.35$ rad/s and the phase margin is 63 deg at $w = 0.1$ rad/s.

18.4.2 Lateral controller

Lateral model

The procedure followed in dealing with the lateral model is analogous to the one used with the longitudinal model.

A linear model is generated from the same trimmed condition used to obtain the linearised longitudinal model. The actuator dynamics have been added to the linear model by augmenting it with corresponding states. Also, we added the two integrated error states and a 0.10 s delay with a first order Padé approximation.

Inner loop controller design

Table 18.6 shows the eigenstructure chosen. The state components are given in the first column, where X_A is the state corresponding to the first order aileron deflection model and X_R the state corresponding to the first order rudder deflection model.

Mode	Dutch roll	Spiral	Roll Sub.	Heading	$\int\beta$	$\int\chi$
Eigenvalues	$-0.8 \pm 0.6i$	-0.4	-1	-0.8	-1.5	-1.4
p	0 0	x	1	x	0	x
r	1 x	x	0	x	x	x
ϕ	0 0	1	x	x	0	x
ψ	x x	x	x	1	x	x
v_B	x 1	0	0	0	x	0
X_A	x x	x	x	x	x	x
X_R	x x	x	x	x	x	x
Delay δ_a	x x	x	x	x	x	x
Delay δ_r	x x	x	x	x	x	x
$\int\beta$	x x	x	x	x	1	x
$\int\chi$	x x	x	x	x	x	1

Table 18.6: Desired eigenstructure of the lateral closed-loop system

The resulting gain is:

$$LatK_{in} = \begin{bmatrix} -3.6246 & 1.7016 & 2.9057 & 3.0480 & 13.1933 & 0.6869 & 2.2288 \\ -1.5216 & -0.0782 & 2.4251 & -0.2268 & 1.0320 & -0.7237 & 0.1820 \end{bmatrix}$$

Loop stability margins

The results obtained at the actuator inputs and at the sensor outputs are summarised in Table 18.7 and Table 18.8, respectively. Figures 18.5 and 18.6 show the singular values plots of the sensitivity functions.

Function	$\overline{\sigma}$	ω	$K_m = 1/\overline{\sigma}$	Gain margin (dB)	Phase margin (deg)
S	1.43	0.65	0.70	[-4.6,10.4]	±40.8
T	1.18	0.21	0.85	[-16.2,5.3]	±50.0
$S+T$	2.19	0.46	0.46	[-8.6,8.6]	±49.2

Table 18.7: Lateral inner loop stability margins at the inputs

Function	$\overline{\sigma}$	ω	$K_m = 1/\overline{\sigma}$	Gain margin(dB)	Phase margin (deg)
S	1.71	0.50	0.59	[-4.0,7.7]	±34.1
T	1.01	0.04	0.99	[-43.3,6.0]	±59.5
$S+T$	2.19	0.46	0.46	[-8.6,8.6]	±49.2

Table 18.8: Lateral inner loop stability margins at the outputs

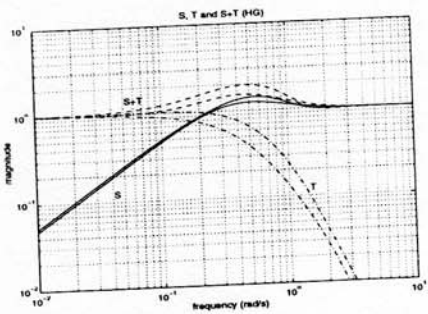

Figure 18.5: Lateral inner loop singular values of the input sensitivity functions

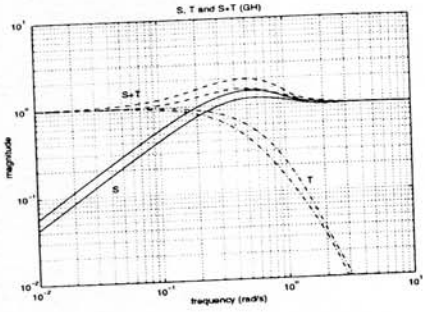

Figure 18.6: Lateral inner loop singular values of the output sensitivity functions

Outer loop controller design

Choosing $LatK_o = 0.001$, the gain margin for the outer loop is 13.9 dB at $w = 0.29$ rad/s and the phase margin is 63.9 deg at $w = 0.08$ rad/s. The slower roots are $-0.11 \pm 0.10i$ that have a rise time of 15 s and a setting time of 44 s. Therefore, the transient specifications for a lateral deviation step command are met.

Detailed response to an engine failure for airspeed and angle of attack has been given in the previous section.

18.5.4 Non-linear simulation under moderate turbulence conditions

We will give an analysis of the non-linear systems under moderate turbulence conditions. The spectra of the turbulence we used in the simulations are described in chapter 14 (§14.2.6).

Figure 18.11 shows actuator behaviour. All the requirements on the mean of actuators are fulfilled. Moreover, all RMS values are less than the limits (the specified values are given in parentheses):

- The mean aileron rate is 0.42 deg/s (< 8.25 deg/s) with a RMS of 7.30 deg/s
- The mean tailplane rate is 0.12 deg/s (< 5 deg/s) with a RMS of 1.03 deg/s
- The mean rudder rate is 0.08 deg/s (< 8.25 deg/s) with a RMS of 1.97 deg/s
- The mean throttle rate is 0.09 deg/s (< 0.24 deg/s) with a RMS of 1.50 deg/s

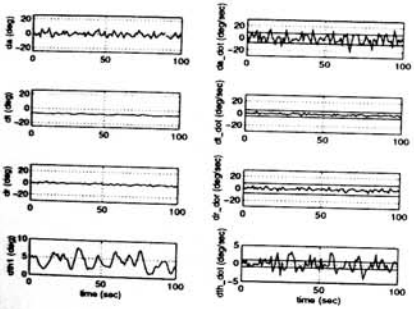

Figure 18.11: Control activity under moderate turbulence conditions

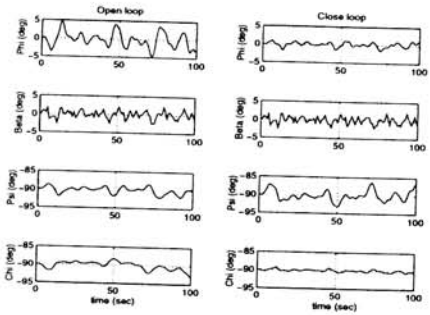

Figure 18.12: Responses under moderate turbulence conditions of angles ϕ, β, ψ and χ

Figure 18.12 shows in open and closed-loop, the roll angle ϕ, the sideslip angle β, the heading angle ψ and the inertial track angle χ under these moderate turbulence conditions. In closed-loop, ϕ always remains within the specified limit of 5 deg. Table 18.9 shows the RMS values of the errors in open and closed-loop. The closed-loop values of ϕ, β and χ are less than their corresponding open-loop values, however the RMS of ψ is higher in closed-loop than in open-loop.

	ϕ	β	ψ	χ
Open loop RMS (deg)	2.04	1.06	0.89	0.97
Closed loop RMS (deg)	0.65	0.96	1.45	0.28

Table 18.9: RMS of the errors in angles ϕ, β, ψ and χ in open and closed-loop

18.5.5 Non-linear simulations observing robustness criteria

Figures 18.13-18.15 show the simulation results obtained at the nominal, minimum and maximum values of time delay, mass and centre of gravity, all cases at the design airspeed of 80 m/s, giving a set of 81 simulations. In the plots, the angles are given in radians, the displacements in meters and the velocities in m/s.

Figure 18.13 shows the lateral step response and the altitude step response. We can see that there is very little control activity, there are almost no overshoots and the settling times are well below the specified values.

Figure 18.14 shows the airspeed-altitude cross-coupling. We can see that the deviations are always within the limits.

Figure 18.15 shows the roll and heading angles at engine failure. In all cases the performance criteria are fulfilled: the roll angle never exceeds 10 deg and its steady state deviation does not exceed 5 deg; the heading rate is always well below the specified 3 deg/s, and the sideslip angle is quickly minimised.

In [52], the simulation results can been found for the inner loop response to heading and flight path angle steps commands, and for air speed step and wind step responses. With respect to the inner loop response to heading and flight path angle steps, in all cases the overshoot is lower than the specified 5 % and the settling time is less than the specifications. Regarding the airspeed step and wind step response, all the performance criteria are fulfilled in the airspeed command. The response to a wind step has three different characteristics which correspond to the three different values of the mass which have been considered. In case of minimum and maximum mass values, the deviation in airspeed is larger than 2.6 m/s after 15 s of the step, and in case of nominal mass value the specification is fulfilled.

In [52], the simulation results obtained for all possible worst conditions of time delay, mass and centre of gravity, at a speed of 63.7 m/s and at maximal flap speed (90 m/s) can also be found.

The worst results are obtained in the engine failure at 63.7 m/s, with minimum mass and with $\Delta x = 0.31\bar{c}$. Consequently, a new set of controller gains was computed using the linearised model at 63.7 m/s velocity, but without changing the rest of the trimming parameters, and with the same eigenstructure as before. The resulting controller and simulation results, obtained by making use of this controller when simulating at 63.7 m/s and for the worst condition of time delay, mass and centre of gravity, are given in [52].

Similar performance and robustness results to those obtained with the controller designed at the original speed of 80 m/s are obtained, thus gain schedul-

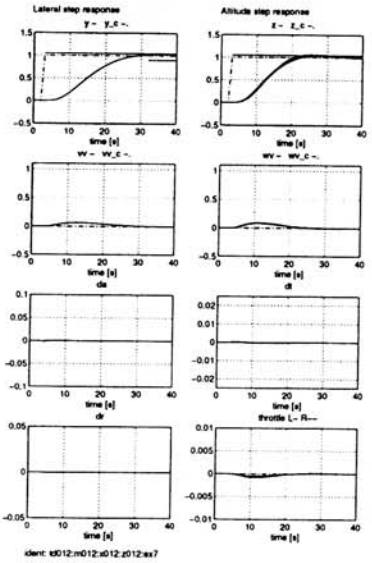

Figure 18.13: Lateral and altitude step response at the design airspeed

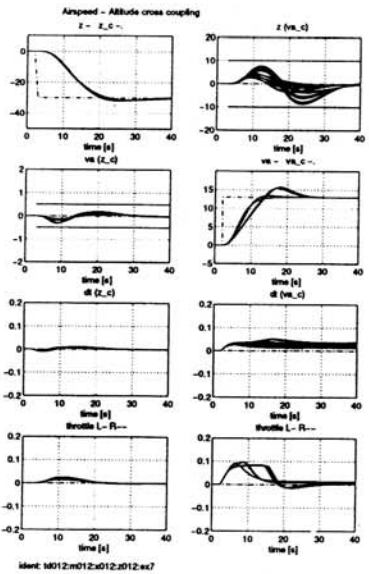

Figure 18.14: Airspeed-altitude cross coupling at the design airspeed

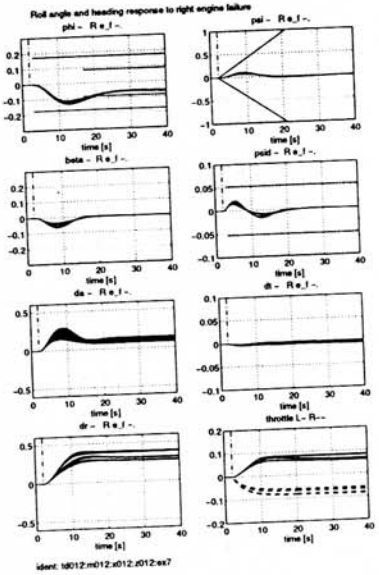

Figure 18.15: Roll angle and heading response to right engine failure at the design airspeed

ing with respect to velocity should be used.

18.6 Results of the automated evaluation procedure

This section presents the results of the evaluation procedure, as proposed in §14.3.3 consisting of a landing approach.

Segment I

Figure 18.16 shows the performance of the controller in this segment, and it can be seen that the lateral deviation is always less than 20 m. Therefore, the controller complies with the corresponding specification. Moreover, the four plots are almost the same, which means small sensitivity to time delay and to horizontal centre of gravity variations.

Segment II

Figure 18.17 gives the behaviour of the model in this manoeuvre. It can be seen that the trajectory of the model surpasses the bounds marked in the plots but the lateral deviation never exceeds the maximum value of 200 m and at the end the lateral deviation is close to zero. The lateral acceleration never surpasses

the maximum allowable value (see Figure 18.9). Moreover, the model has a very smooth turn, fulfils all the performance design criteria and our attempts to have a trajectory within the bounds diminished the stability margins, so we accepted it as is.

Segment III

Figure 18.18 represents the behaviour of the model in the descent phase. It can be seen that the trajectories of the model surpass the bounds marked in the plots although the vertical deviation never exceeds the maximum value of 20 m and at the end of the segment the deviation is close to zero. In Figure 18.10 we can see that the speed variation is well below the allowed 4 m/s. Moreover, the model has a very smooth transition during the entire segment, although the vertical acceleration is a little bit high at some points. We can see in Figure 18.9 that the vertical acceleration slightly surpasses the maximum allowed value. This is reflected in the comfort index in Table 18.10. Since the rest of the design criteria are fulfilled and our attempt to diminish this value produces worse results, we accepted it.

Segment IV

Figure 18.19 shows the behaviour of the model in this segment. It can be seen how the trajectories fall inside the bounds during the entire segment. The rest of the specifications are fulfilled by the controller.

Numerical results

Table 18.10 summarises the results as obtained by the controller along the landing approach. For full details see chapter 14. In general the results are good, except for the comfort criterion in Segment III. The problem with the comfort has already been explained. It is basically due to a small high level of the vertical acceleration.

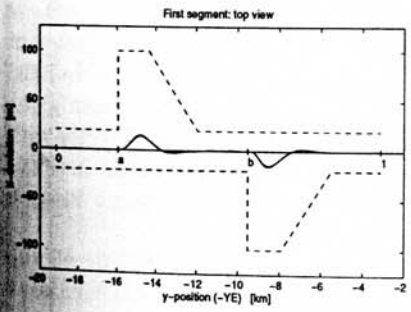

Figure 18.16: Segment I: The effect of engine failure with bounds

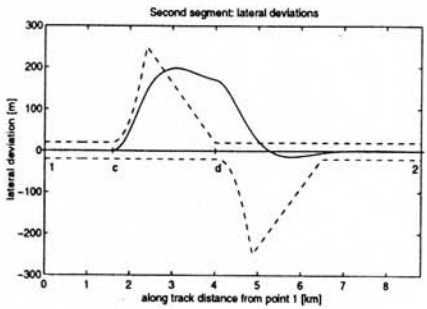

Figure 18.17: Segment II: Lateral deviations during the 90 degrees turn with bounds

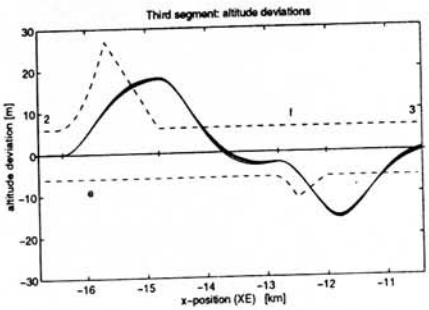

Figure 18.18: Segment III: Vertical deviations during the -6 and 3 degrees glidslope with bounds

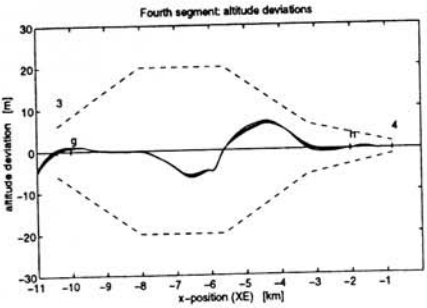

Figure 18.19: Segment IV: Vertical deviations during the final approach with bounds

	Segm. I	Segm. II	Segm. III	Segm. IV	Total
Performance	0.0764	0.4964	0.3285	0.1905	0.2730
Perf. Dev.	0.0309	0.0161	0.4926	0.1873	0.1817
Comfort	0.5432	0.7340	1.1808	0.4674	0.7314
Safety	0.0038	0.0382	0.0070	0.0345	0.0209
Power	0.0037	0.0027	0.0150	0.0309	0.0131

Table 18.10: Numerical results of the evaluation procedure

18.7 Conclusions

In this chapter the eigenstructure method has been applied to the RCAM benchmark problem.

The design was completed by making use of the classical approach. This consists of splitting up the controller into two parts, a longitudinal and a lateral controller, and in using a standard inner-outer loop control structure. In every inner loop the feedback outputs, command signals and integrated outputs have been chosen guided by the design specifications. For both inner loops a constant gain feedback matrix has been calculated using the eigenstructure technique. This method allows the designer to satisfy directly performance criteria given in terms of damping, settling time and decoupling, but not to cope directly with system uncertainties. However, the eigenstructure was chosen in an iterative way, so that good stability margins were obtained. In both outer loops a constant scalar gain has been used.

When analysing the controller with the non-linear model (§18.5) all the design criteria are fulfilled, but the maximum vertical acceleration is surpassed in certain conditions and the RMS of the heading angle error in closed-loop is greater than in open-loop.

Good robustness results are obtained with respect to variations of the mass, centre of gravity and transport time delay. However, gain scheduling should be used with respect to velocity since bad results are obtained with speed

variations, mainly for the engine failure case, as explained in §18.5.

The results obtained in the automatic evaluation procedure demonstrate good good fulfillment of all of the design criteria except the comfort criteria. In our design this is due to the fact that the vertical acceleration cannot be diminished without violating other performance criteria.

The selection of a *good* eigenstructure follows an iterative process that can be time consuming. The process could be shortened if some optimisation method were used. Without any optimisation process, doubts about how good the controller is will always remain.

Lecture Notes in Control and Information Sciences 224

Jean-François Magni, Samir Bennani and Jan Terlouw (Eds)

Robust Flight Control

A Design Challenge

GARTEUR

Springer